Journal of Molecular Liquids 221 (2016) 1022–1028

Contents lists available at ScienceDirect

Journal of Molecular Liquids

journal homepage: www.elsevier.com/locate/molliq

Design and synthesis of amino acid appended azo dye hybrid: Characterization, solvatochromic and quantum-chemical calculations using experimental and theoretical approach

Tej Varma Y [a], Devesh S. Agarwal [b], Amrit Sarmah [c], Yukti [d], Rajeev Sakhuja [b], Debi D. Pant [a,*]

[a] Department of Physics, Birla Institute of Technology and Science (BITS) Pilani, Pilani 333031, Rajasthan, India
[b] Department of Chemistry, Birla Institute of Technology and Science (BITS) Pilani, Pilani 333031, Rajasthan, India
[c] Department of Chemistry, Ben-Gurion University, Negev, Israel
[d] Department of Chemical Engineering, Birla Institute of Technology and Science (BITS) Pilani, Pilani 333031, Rajasthan, India

ARTICLE INFO

Article history:
Received 23 February 2016
Received in revised form 13 June 2016
Accepted 13 June 2016
Available online 21 June 2016

Keywords:
Azo dye
Dipole moment
Solvatochromic shift

ABSTRACT

Amino acid appended azobenzene hybrid was synthesized and characterized using Spectroscopic techniques like ^{1}H NMR, ^{13}C NMR, FT-IR and Mass spectrometry analysis and its optical properties were investigated using UV–vis absorption and fluorescence spectroscopy in solvents of different polarity. Based on solvent refractive index and relative permittivity, by using the theory of solvatochromism, the excited-state (μ_e) and ground-state (μ_g) dipole moments was determined for (E)-4-((4-(heptyloxy)phenyl)diazenyl)benzyl((benzyloxy)carbonyl)glycinate (Gly-Azo-O7) based on the variation of Stokes shift as an effect of various solvent's. A bathochromic shift observed in absorption and emission spectra with increasing solvent polarity, which implied that the transition involved is $\pi \rightarrow \pi^*$. The ground state and excited state dipole moments were also calculated and compared using experimental and DFT calculations.

1. Introduction

Azo dyes are one of the important class of photoresponsive materials due to their inherent property to undergo *cis-trans* isomerization and also an important class of colorants [1]. But there are few aspects which require a deeper study, especially amino acid derived azo dye derivatives. Amino acids are the most abundant materials present which make them most versatile materials for the synthesis of functional materials which can be used for various application in materials as well as in pharmaceutical field [2].

The photophysical properties of the azo dye derivatives have been widely explored [3]. In this context photophysical studies of the molecules especially estimation of excited and ground state dipole moment calculations and effect of different solvent polarity remains an area of great interest and have gained tremendous advancement due to their wide range of application in various fields. For instance, fluorescent probe method is now extensively used for studying cells, proteins, and tissues [4,5]. Hence in order to understand their structure it is important we use solvatochromic shifts method for the estimation of the ground and excited state dipole moments of a molecule [6–17]. Thus the local dielectric constant may be determined by these equations from the spectral position of the electronic spectra [18–23] based on the knowledge of the dipole moments. Thusly solvents effect on the steady state spectral properties of organic fluorophores have been a subject of ongoing investigation [24–29] as they also have applications in the field of photophysics and photochemistry.

Estimation of ground and singlet excited-state dipole moments are based on the spectral shift caused externally by electrochromism or internally by solvatochromism. Methods such as electric polarisation of fluorescence [30] and electric dichroism [31] are generally considered to be very accurate; however, their use is limited and has so far been restricted to rather small or simple molecules. Hence solvatochromism is a widely accepted and incomplex experimental method [30–35], as no external field is used [36,37]. Thus providing a reliable method [38–43] to estimate ground and excited state dipole moment based on the shift of the absorption and fluorescence maxima in various media. Thus insight of electronically excited dipole moments of organic molecules is generally useful in the derivation of parameters like molecular polarizability in non-linear optical materials (NLO) [44] using electro-optic methods and also in the design of new molecules.

In continuation to our research to study the ground and excited state dipole moment of different molecular systems we have reported the study on excited state and ground state dipole moment of quinine sulfate monocation (QS^+) [45], quinine sulfate dication (QS^{2+}) [46], quinidine (Qd^+), quinidine dication (Qd^{2+}) [47], 6-methoxyquinoline 6MQ [35], and coumarin derivative [N-(2-oxo-2H-chromen-4-yl)imino]triphenyl-phosphorane [48] and (S)-(1-((7-hydroxy-2-oxo-

* Corresponding author.
E-mail address: ddpant@pilani.bits-pilani.ac.in (D.D. Pant).

http://dx.doi.org/10.1016/j.molliq.2016.06.045
0167-7322/

2H-chromen-4-yl) methyl)-1H-1,2,3-triazol-4-yl)methyl 2-(((9H-fluoren-9-yl)methoxy) cabonylamino)-3-phenylpropanoate [49], cinchonidine and cinchonidine dications [50] using solvatochromic shift method. We observed a large change in dipole moment of these molecules in the excited state compared to the ground state.

There have been reports on the Solvatochromic and calculation of the ground state and excited state dipole moment calculation of the azo dyes [51–54], but there is no report on the Solvatochromic study of the amino acid appended azobenzene derivatives. In the view of the above discussion we here in report the synthesis of amino acid appended azo dye hybrid (Gly-Azo-O7) and estimation of its ground state and excited state dipole by the solvatochromic shift method using Bakhshiev [55] and Bilot–Kawski [56,57] correlations and theoretically using Density Function Theory (DFT).

2. Experimental

2.1. Materials

All the chemicals were purchased from Sigma-Aldich, Alfa Aesar, and Spectrochem India Pvt. Ltd. and used without further purification. All the solvents used were HPLC grade or AR (purchased from Alfa Aesar). Ethyl 4-aminobenzoate (1) and Phenol (2) were purchased from commercial source and compound 3,was synthesized according to reported protocol (Scheme 1) [58] and was characterized using ^{1}H NMR and ^{13}C NMR. (for the spectral data please see the supporting information).

2.2. Instrumentation

Nuclear magnetic resonance spectra (NMR), the ^{1}H NMR were recorded on Bruker 400 MHz spectrometer and ^{13}C NMR spectrometer was recorded on Bruker AMX 100 MHz solid state NMR spectrometer. Melting points were determined on a capillary point apparatus equipped with a digital thermometer and are uncorrected. Reactions were monitored by using thin layer chromatography (TLC) on 0.2 mm silica gel F254 plates (Merck). High resolution mass spectrometry (HRMS) was performed with a waters synapt G2 HDMS instrument using time-of-flight (TOF-MS) with ESI/APCI- hybrid quadrupole. FT-IR was taken on ABB Bomen MB 3000 FTIR for gelator and freeze dried gels, using KBr disk technique. Absorption spectra were taken with the help of dual beam JASCO V-570 UV/Vis/NIR spectrophotometer and fluorescence spectra were recorded with the help of Shimadzu, RF-5301PC spectrofluorometer. The data were analyzed using related software. The spectral shifts obtained with different sets of samples were identical in most of the cases and values were within ±1.0 nm. Data were analyzed and were fitted to a straight line using Origin 6.1 software. Density of the probe was estimated by ACD/Chemsketch software. The concentration of Gly-Azo-O7 in all the solutions prepared in different solvents was 10^{-4} M.

2.3. Synthesis

2.3.1. Synthesis of ethyl (E)-4-((4-(heptyloxy)phenyl)diazenyl)benzoate (4, Scheme 2)

To the stirred solution of 3 (1 g, 3.5 mmol) in acetone K_2CO_3 (1.2 g, 8.7 mmol) was added at 0 °C. the reaction mixture was stirred for 15mins at 0 °C after which 1-bromo heptane (0.75 g, 4.2 mmol) was added and the reaction was refluxed for 16 h. The completion of the reaction was monitored by TLC. After the completion of the reaction, the reaction mixture concentrated under reduced pressure and water (50 mL) was added. The formed precipitate was filtered under suction to yield crude product which was recrystallized using ethanol to yield pure product as orange solid (1.02 g, 84.2%).

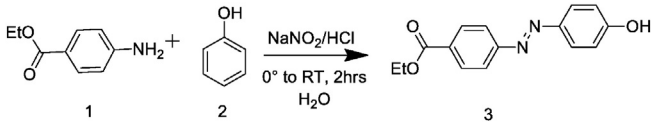

Scheme 1. Synthesis of (E)-4-((4(heptyloxy)phenyl)diazenyl)benzyl((benzyloxy)carbonyl) glycinate (Gly-Azo-O7).

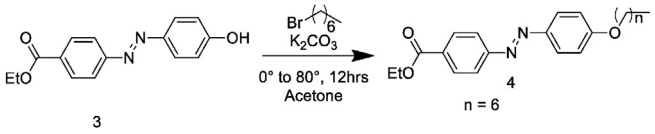

Scheme 2. Synthesis of ethyl (E)-4-((4-heptyloxy)phenyl)diazenyl)benzoate.

^{1}H NMR (400 MHz, $CDCl_3$) δ 8.20 (d, J = 8.7 Hz, 2H), 7.94 (dd, J = 15.6, 8.9 Hz, 4H), 7.04 (d, J = 9.0 Hz, 2H), 4.43 (q, J = 7.1 Hz, 2H), 4.07 (t, J = 6.6 Hz, 2H), 1.90–1.80 (m, 2H), 1.55–1.47 (m, 2H), 1.45 (t, J = 7.1 Hz, 3H), 1.42–1.29 (m, 6H), 0.93 (t, J = 6.9 Hz, 3H). ^{13}C NMR (101 MHz, $CDCl_3$) δ 166.2, 162.3, 155.3, 146.8, 131.5, 130.5, 125.2, 122.3, 114.8, 68.4, 61.2, 31.8, 29.2, 29.1, 25.9, 22.6, 14.4, 14.1. FT-IR (KBr, υ, cm^{-1}) 2916, 2847, 1713, 1504, 1466, 1295, 841.

2.3.2. Synthesis of (E)-(4-((4-(heptyloxy)phenyl)diazenyl)phenyl)methanol (5, Scheme 3)

To a solution of LAH (0.154 mg, 4.07 mmol), in dry THF (20 mL) at 0 ° C, to this solution 4 (0.500 mg, 1.35 mmol). The reaction mixture was stirred at room temperature for 2 h. after completion of the reaction, the reaction was cooled to 0 °C and quenched by adding 1 N NaOH solution (30 mL). Subsequently ethyl acetate (20 mL) was added and the reaction was filtered through celite and extracted using ethyl acetate (20 mL × 2). The organic layer was dried over sodium sulfate and concentrated under reduced to give crude product which was recrystallized using ethanol to give pure product as orange solid (371 mg., 83.8%).

Mp: 118.5–119 °C ^{1}H NMR (400 MHz, $CDCl_3$) δ 7.88 (dd, J = 14.5, 8.6 Hz, 4H), 7.48 (d, J = 8.3 Hz, 2H), 6.99 (d, J = 9.0 Hz, 2H), 4.76 (s, 2H), 4.03 (t, J = 6.6 Hz, 2H), 1.84–1.78 (m, 2H), 1.51–1.41 (m, 2H), 1.37–1.27 (m, 7H), 0.89 (t, J = 6.8 Hz, 3H). ^{13}C NMR (101 MHz, $CDCl_3$) δ 161.8, 152.3, 146.8, 143.1, 127.5, 124.8, 122.8, 114.7, 68.4, 64.9, 31.8, 29.4, 29.3, 26.0, 22.7, 14.1. FT-IR (KBr, υ, cm^{-1}) 3055, 2924, 2854, 1713, 1597, 1466, 1281, 1250, 1142, 841.

2.3.3. Synthesis of (E)-4-((4-(heptyloxy)phenyl)diazenyl)benzyl ((benzyloxy)carbonyl)glycinate (Gly-Azo-O7, 7, Scheme 4)

To the stirred solution of Cbz-glycine (6) (269 mg, 1.28 mmol) in DCM (20 mL), DMAP (13.07 mg, 0.107 mmol) was added at 0 °C and subsequently EDC.HCl (307.67 mg, 1.6605 mmol.) and HOBt (163.86 mg, 1.07 mmol.) was added. The reaction mixture was stirred for 15 min. at 0 °C, after which, 5 (350 mg, 1.07 mmol.) was added and the reaction was stirred at room temperature for 6–8 h. The completion of the reaction was monitored by TLC. After the completion of the reaction, the reaction mixture was diluted with water and extracted. Organic layer was separated and dried over anhydrous sodium sulfate and evaporated under reduced pressure to give crude product which was recrystallized using ethanol to yield pure product 7 (442 mg, 78.8%) as orange solid. Synthesis of Gly-Azo-O7, 7 is shown in Scheme 1.

^{1}H NMR (400 MHz, $CDCl_3$) δ 7.91 (dd, J = 17.9, 8.7 Hz, 4H), 7.49 (d, J = 8.3 Hz, 2H), 7.41–7.32 (m, 5H), 7.03 (d, J = 9.0 Hz, 2H), 5.36–5.27 (m, 1H), 5.27 (s, 2H), 5.16 (s, 2H), 4.07 (dd, J = 12.1, 5.9 Hz, 4H), 1.89–1.80 (m, 2H), 1.55–1.46 (m, 2H), 1.43–1.30 (m, 6H), 0.93 (t, J =

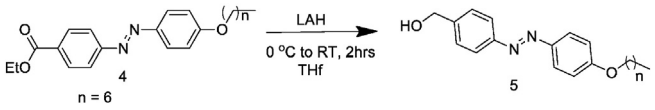

Scheme 3. Synthesis of (E)-(4-((4-(heptyloxy)phenyl)diazenyl)phenyl)methanol.

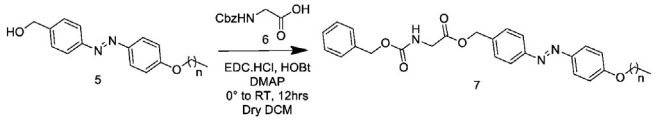

Scheme 4. Synthesis of (E)-4-((4-(heptyloxy)phenyl)diazenyl)benzyl ((benzyloxy) carbonyl)glycinate.

6.9 Hz, 3H). ^{13}C NMR (101 MHz, $CDCl_3$) δ 169.8, 161.9, 156.3, 152.8, 146.8, 137.1, 136.2, 129.0, 128.6, 128.3, 128.2, 124.9, 122.8, 114.7, 68.4, 67.2, 66.8, 42.9, 31.8, 29.2, 29.1, 26.0, 22.6, 14.1. HRMS (ESI): *m/z* $[M + H]^+$ calcd for Chemical Formula: $C_{30}H_{36}N_3O_5$: 518.2654 found: 518.2631; FT-IR (KBr, υ, cm^{-1}) 3340, 2932, 2862, 1751, 1690, 1528, 1250, 1157, 841.

2.4. Experimental calculations of ground and excited state dipole moments

The movement of absorption and fluorescence spectra of a solute molecule is allied to its reciprocal action with the solvent. These interactions can be non-specific, when they depend only on multiple and polarizability properties of solute and solvent molecules. The bulk dielectric constant (**ε**), refractive index (**η**) of the solvent and spectroscopic shifts can be used, for the estimation of ground and excited state dipole moments of the molecule, since they strongly affect the dipole moment. The dipole moment of a molecule in the excited-state is determined by the effect of an electric field (internal or external) on its spectral band position. On the basic of quantum-mechanical second order perturbation theory, Bilot and Kawski [56,57] derived two expressions for solvatochromism as a function of refractive index and permittivity of various solvents, which are given as Bakhshiev's formula [55]

$$\bar{\nu}_a - \bar{\nu}_f = S_1 F_1(\varepsilon,\eta) + \text{const.} \quad (1)$$

Here $\bar{\nu}_a$ and $\bar{\nu}_f$ are the wavenumbers of the absorption and emission maxima respectively.

F_1 the bulk solvent polarity function and S_1 the slope are defined as follows:

$$F_1(\varepsilon,\eta) = \frac{2\eta^2+1}{\eta^2+2}\left[\frac{\varepsilon-1}{\varepsilon+2} - \frac{\eta^2-1}{\eta^2+2}\right] \quad (2)$$

and

$$S_1 = \frac{2\left(\mu_e - \mu_g\right)^2}{hca_0^3} \quad (3)$$

here we denote the Planck's constant, c is the velocity of light in vacuum, μ_g is the dipole moment in the excited singlet state, a_0 is the Onsager cavity radius, ε is the solvent dielectric constant and η is the solvent refractive index.

Bilot–Kawski formula [56,57]

$$\frac{\bar{\nu}_a + \bar{\nu}}{2} = -S_2 F_2(\varepsilon,\eta) + \text{const.} \quad (4)$$

Here the meaning of symbols is same as given above except for F_2 and S_2 which are defined as follows

$$F_2(\varepsilon,\eta)\frac{2\eta^2+1}{2(\eta^2+2)}\left[\frac{\varepsilon-1}{\varepsilon+2} - \frac{\eta^2-1}{\eta^2+2}\right] + \frac{3}{2}\left[\frac{\eta^4-1}{(\eta^4+2)^2}\right] \quad (5)$$

and

$$S_2 = \frac{2\left(\mu_e^2 - \mu_g^2\right)}{hca_0^3} \quad (6)$$

The parameters S_1 and S_2 are the slopes which can be calculated from Eqs. (1) and (4) respectively. Assuming the ground and excited states are parallel, the following expressions are obtained using Eqs. (3) and (6) [27]

$$\mu_g = \frac{S_2 - S_1}{2}\left[\frac{hca_0^3}{2S_1}\right]^{1/2} \quad (7)$$

$$\mu_e = \frac{S_1 + S_2}{2}\left[\frac{hca_0^3}{2S_1}\right]^{1/2} \quad (8)$$

and

$$\mu_e = \frac{|S_1 + S_2|}{|S_2 - S_1|}\mu_g \quad (9)$$

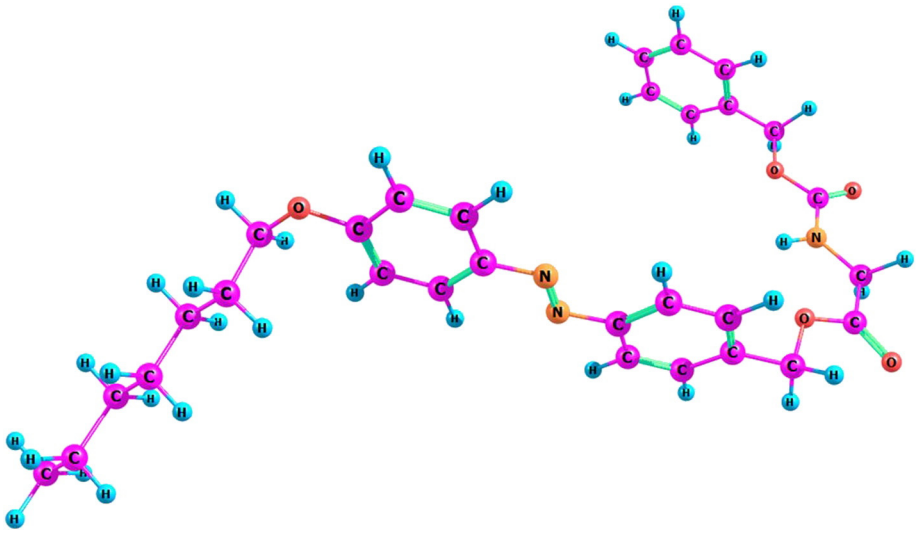

Fig. 1. Gas phase optimized structure of (Gly-Azo-O7) at B3LYP/6–31 + G(d,p) level.

The value of solute cavity radius (a_0) was calculated from the molecular volume according to Suppan's equation [11]

$$a_0 = \left(\frac{3M}{4\pi\delta N}\right)^{1/3} \quad (10)$$

2.5. Computational details

We have used Density Functional Theory (DFT) [59,60] based calculation to compute the ground and excited state dipole moment along with the Onsager radii of the compound Gly-Azo-O7. Gaussian09 program suit [61] is used throughout the calculation. The ground state geometry optimization are performed using B3LYP [62] method and 6–31 + G(d,p) basis sets. Here, incorporation of diffuse function in the basis sets enhanced the accuracy of computational calculations. Subsequently, frequency calculation is also performed at the same level (i.e., B3LYP/6–31 + G(d,p)) to ensure the global minima for optimized structure of the compound Gly-Azo-O7. First excited state TD-DFT calculations are performed on the ground state optimized geometry of the compound at B3LYP/6–31 + G(d,p) level. The solute-solvent interaction is modeled for various solvents using integral equation formalism polarizable continuum model (IEF-PCM) [63] considering the self-consistent reaction field (SCRF) [64] method as implemented in Gaussian09. The cavity is build using UA0 radii. The United Atom Topological Model is implemented on atomic radii of the UFF force field for heavy atoms. The Hydrogen atoms are also considered in the sphere of the heavy atom to which they are attached through covalent bonding interaction. The optimized structure of the compound is reported in Fig. 1. GaussView05 [65] visualization software has been used to generate visual graphics of the theoretical calculations.

3. Result and discussion

3.1. ^{1}H NMR spectra

The ^{1}H NMR spectra of 4 showed in $CDCl_3$ at room temperature showed a clear triplet at δ_H 4.07 indicating the presence of a CH_2 attached to phenolic –OH and presence of a triplet at δ_H 0.93 indicating the presence of a methyl group suggesting that the attachment of the alkyl chain to 3. The ^{1}H NMR spectra of 5 showed a disappearance of quartet at δ_H 4.43 and a triplet at δ_H 1.45 and the appearance of a singlet at δ_H 4.76 indicating the reduction of ester functionality to alcohol. Similarly coupling of *Cbz*-glycine with 5 showed a change in the ^{1}H NMR spectra of 7 indicating the presence of a multiplet of –NH showing successful synthesis of Gly-Azo-O7.

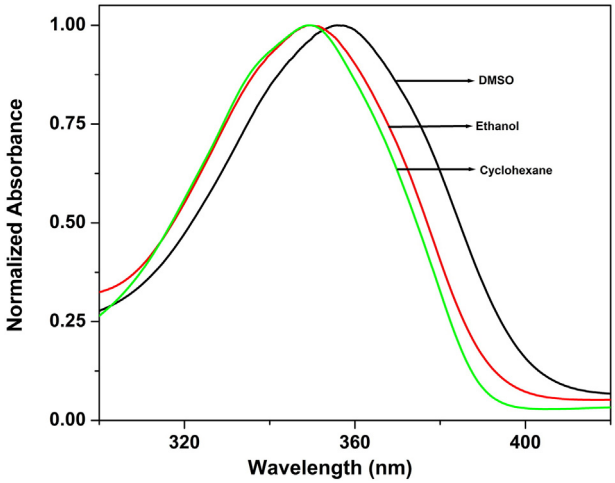

Fig. 2. Normalized absorption spectra of in dimethyl sulfoxide., ethanol and cyclohexane.

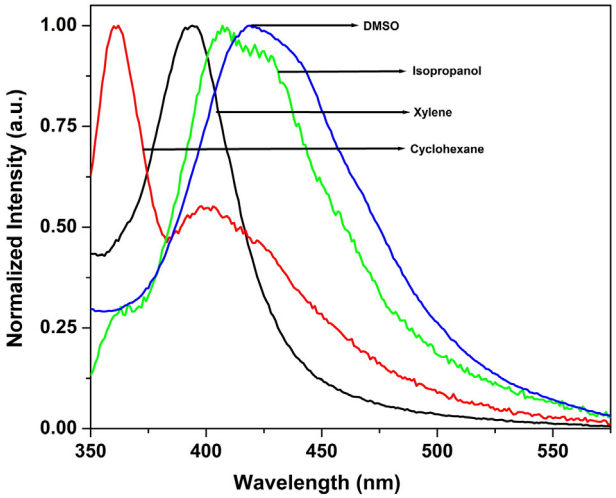

Fig. 3. Fluorescence spectra of in dimethyl sulfoxide, isopropanol, xylene and cyclohexane.

3.2. Solvent effect on the electronic absorption spectra

The steady state absorption was recorded in different organic solvents ranging from protic polar to aprotic polar and to non-polar solvents at room temperature are shown in Fig. 2. The absorption maximum was obtained in the range of 349 nm to 356 nm. The absorption band shows a modest shift (2–7 nm) implying that the solvent effect is negligible for the molecules in the ground state toward solvent polarity. It can also be seen that the first absorption band centered at 349–356 nm are assigned to $\pi \rightarrow \pi^*$ transitions due to the delocalization in aromatic rings.

3.3. Solvent effect on the electronic emission spectra

The fluorescence spectra for Gly-Azo-O7 in different organic solvents are shown in Fig. 3. The investigated compound shows single emission band in all solvents except for cyclohexane. The low intensity emission band observed in cyclohexane around 400 nm can be ascribed to partly forbidden $n \rightarrow \pi^*$ electronic transition which are due to the interaction of lone pair of nitrogen atoms with the solvent. The first emission band of Gly-Azo-O7 is in the range of 362 nm to 423 nm. As we increase the solvent polarity from cyclohexane to methanol to DMSO the emission maximum are shifted to longer wavelengths from 362 nm to 413 nm to 423 nm respectively. The bathochromic shift from 362 nm to 423 nm corresponding to 61 nm shift confirms a $\pi \rightarrow \pi^*$ electronic transitions which are borne out from the conjugation between the azo bridge (-N = N-) and aromatic ring system [66–68]. On increasing the solvent polarity the stoke shift value enhances from 1012 cm^{-1} to 4449 cm^{-1} for cyclohexane to DMSO respectively, thus the magnitude of stokes shifts is also a indicative of intramolecular

Table 1
Different solvent parameters and spectral data of Gly-Azo-O7 in different solvents.

Solvent	ε	η	F_1	F_2	$\bar{\nu}_a - \bar{\nu}_f$ (cm^{-1})	$\frac{\bar{\nu}_a + \bar{\nu}_f}{2}$ (cm^{-1})
DMSO	46.4	1.4780	0.866	0.756	4449	25865
Acetonitrile	37.5	1.3284	0.892	0.680	3916	26589
Methanol	32.7	1.3280	0.887	0.667	4751	26591
Ethanol	24.5	1.3614	0.812	0.652	4170	26535
Isopropanol	20.3	1.3856	0.779	0.651	4058	26599
Ethyl acetate	6.1	1.3724	0.489	0.497	4384	26347
Xylene	2.4	1.5054	0.0277	0.354	2788	26775
Cyclohexane	2.0	1.420	−0.0065	0.284	1012	28131

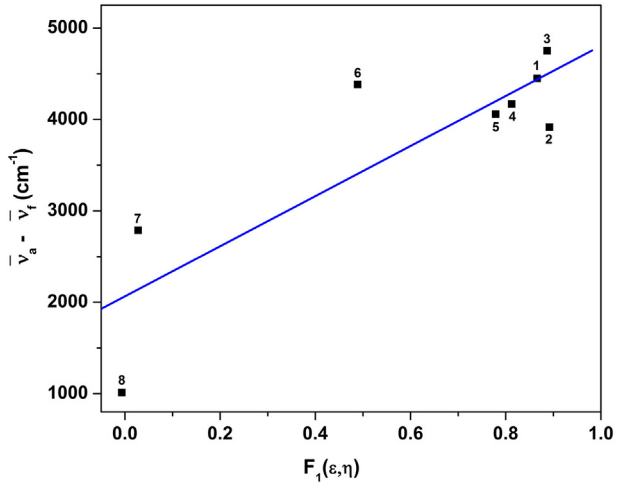

Fig. 4. Plot for Stokes shift versus solvent polarity function F_1.for in (1) DMSO, (2) acetonitrile, (3) methanol, (4) ethanol, (5) isopropanol, (6) ethylacetate, (7) xylene and (8) cyclohexane.

charge transfer. These data implies that the molecule is influences by parameters such as polarity, hydrogen bond donor-acceptor strength. The hypochromic shift associated with decrease in solvent polarity implies that the charge distribution between the ground state and the excited state due to strong intermolecular interactions with polar solvents. Thus reveals that the molecule is more stabilized in the excited state in polar solvents than the ground state implying that the expected excited state dipole moment will be higher.

3.4. Solvation effect on absorption and emission electronic spectra

Solvation effects show that different solvent polarities have various consequences on fluorescence spectra whereas in UV–vis spectra the protic polar nature seems to be of utmost importance. It was also noticed that DMSO cause rising of absorbance in Gly-Azo-O7 compared to other solvents and also exalts the same behavior in fluorescence emission. Such behavior highlights the role of hydrogen bonding between solute and solvent [69] since Kamlet-Taft parameters of these solvents show that DMSO are strong hydrogen bond acceptors. Thus the interaction of amine group with solvent molecules, which act as both hydrogen acceptor/donor groups, can explain the solvation on spectra of Gly-Azo-O7. The increase in solvent polarity can be explained

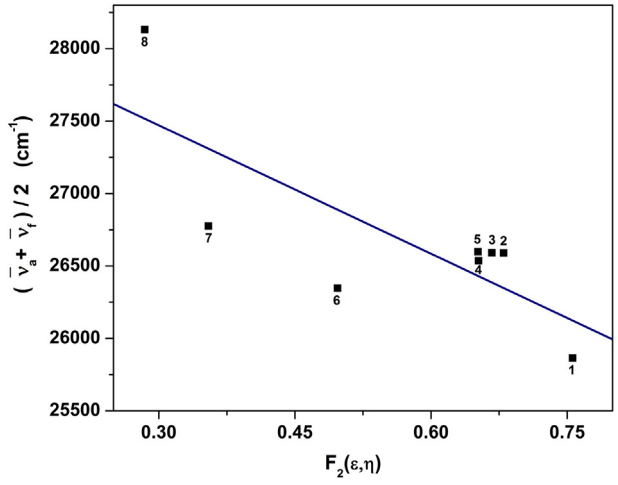

Fig. 5. Plot for arithmetic average of absorption and fluorescence wave numbers versus solvent polarity function F_2 for in (1) DMSO, (2) acetonitrile, (3) methanol, (4) ethanol, (5) isopropanol, (6) ethylacetate, (7) xylene and (8) cyclohexane.

Table 2
Experimentally calculated Dipole moment data of Gly-Azo-O7 in ground and excited states.

Molecule	a_0 (Å)	S_1 (cm^{-1})	S_2 (cm^{-1})	μ_g (D)	μ_e (D)	$\Delta\mu$ (D)	μ_e/μ_g
Name	6.33	2741	−2956	1.74	8.2	6.46	4.71

by the destabilization of secondary amine group (Scheme 1) leading to the stabilization of the planar state initializing hydrogen bonding and π → π stacking in the secondary amine and azo benzene group which causes a constrain in the motion of hydrophobic tale. Solvation of the secondary amine group with hydrogen bond acceptor like DMSO causes planar conformation of Gly-Azo-O7. In this case the lone pair of the nitrogen atom and a hydrogen atom of amine group of the azo benzene unit is involved in hydrogen bonding.

3.5. Experimental calculations of ground and excited state dipole moments

To study the solvatochromism of Gly-Azo-O7, the spectral parameters are found to be correlated by employing Bilot–Kawski and Bakhshiev's linear correlations. To get further insight spectroscopic properties are correlated with relevant solvent polarities scale. Solvent polarity function have been $F_1(\varepsilon, \eta)$,F_2 (ε, η) and spectral shift $\bar{\nu}_a - \bar{\nu}_f$ and $(\bar{\nu}_a - \bar{\nu}_f)/2$ have been tabulated in Table 1 in order to estimate the ground state and excited state dipole moment of the molecule. Thus, Figs. 4 and 5 shows graphs of stokes shifts $\bar{\nu}_a - \bar{\nu}_f$ and $(\bar{\nu}_a - \bar{\nu}_f)/2$ with solvent polarity fuctions $F_1(\varepsilon, \eta)$ and F_2 (ε, η) respectively.

The slopes S_1 and S_2 obtained from the graphs were 2741 and −2956 respectively, are used to obtain the ground and excited state dipole moments in accordance to Eqs. (7) and (8). The solute cavity radius (a_o) was calculated using Eq. (10), a_o was found to be 6.33 Å. The experimental ground and excited state dipole moment are 1.74 (D) and 8.2 (D) respectively and have been summarized in Table 2, this confirms that the dye is more polar in their excited singlet state than in the ground state, which is in agreement with the better stabilization under excitation that is consistent with, stokes shifts data. . Furthermore due to change in electron densities in the ground and excited state the dipole moment is different in these states. Thus it is evident that the excited state dipole moment is higher than that of the ground state dipole moment suggesting that the emission of this dye originates from a state, which is more polar than the ground state, is probably intramolecular charge transfer (ICT) in excited state.

3.6. Theoretical calculations of ground and excited state dipole moments

Theoretically calculated ground and excited state dipole moment values in gas phase as well as four different solvents are reported in Table 3. It is worth mentioning here that, the experimental and theoretical calculations of the excited state dipole moment are in an qualitative

Table 3
Dipole moment (Debye) calculated at the B3LYP/6–31 + G(d,p) level of theory for Gly-Azo-O7.

Solvent	Dielectric constant	Ground state dipole moment (μ_g)[a]	Excited state dipole moment (μ_e)[b]
Gas	–	7.8267	7.6066
Acetonitrile	35.9	9.2146	8.4318
Benzene	2.27	8.5352	8.2718
Cyclohexane	2.01	8.4543	8.1965
Dimethyl sulfoxide	46.4	9.2392	8.9242

[a] μ_g ground state dipole moment values computed at B3LYP/6–31 + G(d,p) level of theory for gas phase and also the same level of theory using IEF-PCM model along with UA0 radii for solvents.

[b] μ_e excited state dipole moment values computed from single point TD-B3LYP/6–31 + G(d,p) level (on the gas phase optimized geometry of the compound) for gas phase and also the same level of theory using IEF-PCM model along with UA0 radii for solvents.

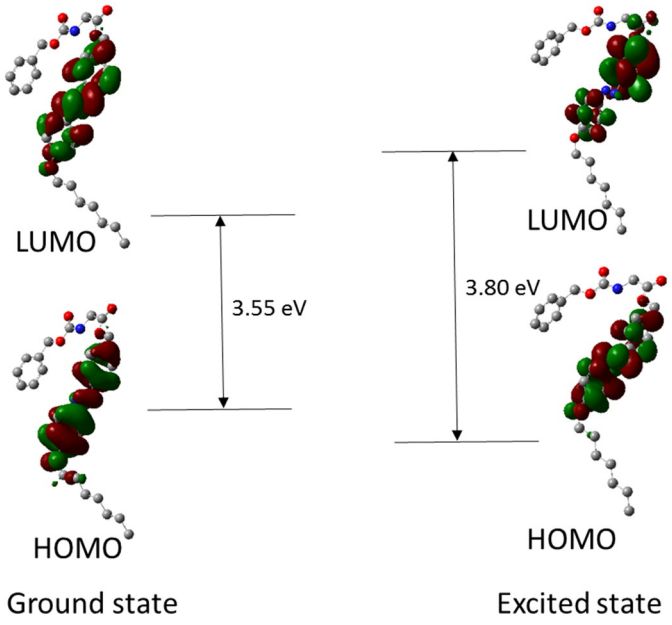

Fig. 6. The gas phase ground and excited state HOMO-LUMO structures of Gly-Azo-O7 at B3LYP/6–31 + G(d,p) level.

agreement with each other in gas and solvent phase. Although, the theoretically obtained ground state dipole moment values are significantly higher than the experimental one, normally, this is a usual theoretical artefact in case of compounds having long hydrocarbon chain. An inherent limitation of DFT formalism (that cannot take care the nonbonding interactions) greatly alters the electronic distribution in the particular system and this became significantly uneven. Perhaps, this attributes virtual increase in the polarity to the system which is quite different from the real one. Again, a poor electron correlation is also responsible for the variation of dipole moment in the system. It is also assumed that the theoretical methods containing higher level of electron correlation will significantly improve the computed dipole moment values. [70] Perhaps, a higher order basis sets is also very essential for the greater accuracy [71].

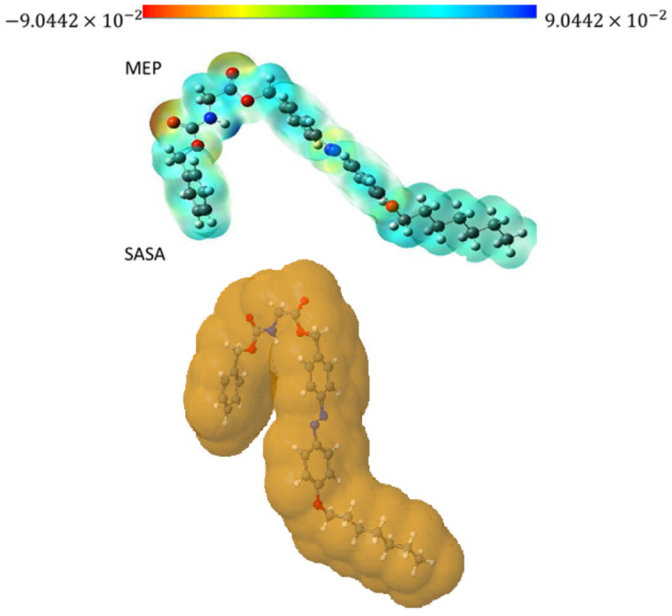

Fig. 7. Visual representations of the computed molecular electrostatic potential (MEP) and solvent accessible surface area (SASA) of Gly-Azo-O7 at B3LYP/6–31 + G(d,p) level.

But, in case of a relatively large system like Gly-Azo-O7, application of higher order method and relatively large size basis sets introduce many fold increases the computational cost. So, at a reasonable computational cost along with moderate accuracy B3LYP (method) and 6–31 + G(d,p) (basis sets) combination produced dipole moment values that are reasonably good in case of qualitative assessment. It is also observed that while moving from gaseous to solvent phases the dipole moment values are increased. It is quite obvious that, in the vicinity of solvent, a sharp increase in the intermolecular solute-solvent interaction leading toward an enhanced of dipole moment values.

With the increase of solvent polarity the value of the dipole moment is also increasing (Table 3). The ground and excited state HOMO-LUMOs are reported in Fig. 6 along with their corresponding energy gaps. We have observed that the HOMO-LUMO energy gap has been slightly increased in the excited state. The molecular electrostatic potential (MEP) along with solvent accessible surface area (SASA) maps are reported in Fig. 7. The colour of the surface in case of MEP indicates the variation of electron density (per unit volume) at different points on the system. The red zone indicates the presence of higher electron density and the lighter zone reflects the electron deficient areas in the molecule.

4. Conclusion

In the present work, we have reported the solvent effect by examining dipole moments of Gly-Azo-O7 in three groups of various solvents viz. non-polar, protic polar and aprotic polar experimentally and thoeritically. A red shift is observed upon increasing the polarity of the solvent indicating a $\pi \rightarrow \pi^*$ transition. We also observed a forbidden $n \rightarrow \pi^*$ transition in emission spectra of solute in cyclohexane. The probe poses higher dipole moment in the excited state (μ_e) compared to the ground state (μ_g) indicating that the probe in excited state is more polar than in the ground state. And the values of excited state dipole moment are in agreement experimentally and theoretically.

Acknowledgment

We acknowledge Department of Science and Technology (DST), New Delhi for major research project to D.D.P. T.V.Y thanks Birla Institute of Technology and Sciences, Pilani Campus for Research fellowship. The author DA is thankful to DST, New Delhi for JRF, RS is thankful to DST, New Delhi for major research project.

Appendix A. Supplementary data

^{1}H NMR and ^{13}C NMR can be obtained free of charge from the online version, at doi: http://dx.doi.org/10.1016/j.molliq.2016.06.045.

References

[1] (a) H. Zollinger, Colour Chemistry, VCH, Weinheim, 1987;
(b) G.S. Uscumlic, D.Z. Mijin, N.V. Valentic, V.V. Vajs, B.M. Susi (Eds.),Chem. Phys. Lett. 397 (2004) 148.
[2] (a) M.S. Dillingham, M.I. Wallace, Org. Biomol. Chem. 6 (2008) 3031;
(b) H. Mihara, S. Lee, Y. Shimohigashi, H. Aoyagi, T. Kato, N. Izumiya, T. Costa, FEBS Lett. 193 (1985) 35.
[3] S.S. Babu, V.K. Praveen, A. Ajayaghosh, Chem. Rev. 114 (2014) 1973–2129 (and references therein).
[4] J.R. Lakowicz, Principles of Fluorescence Spectroscopy, Plenum Press, New York, 1999.
[5] G.E. Dobretsov, Fluorescent Probes for Studying Cells, Membranes and Proteins, Nauka, Moscow, 1989 (in Russian).
[6] E.G. McRae, J. Phys. Chem. 61 (5) (1957) 562–572.
[7] M.B. Ledger, P. Suppan, Spectrochim. Acta 23A (3) (1967) 641–653.
[8] P. Suppan, C. Tsiams, Spectrochim. Acta 36A (4) (1980) 971–974.
[9] C.-L. Gáspár, I. Panea, I. Bâldea, Dyes Pigments 76 (2) (2008) 455–462.
[10] L.S. Prabhumirashi, Spectrochim. Acta 39A (1) (1983) 91–92.
[11] P. Suppan, Chem. Phys. Lett. 94 (3) (1983) 272–275.
[12] N.H. Ayachit, D.K. Deshpande, M.A. Shashidhar, K. Suryanarayana Rao, Spectrochim. Acta 42A (5) (1986) 585–587.
[13] C.N.R. Rao, S. Singh, V.P. Senthilanthan, Chem. Soc. Rev. 5 (1976) 297–316.

[14] N.H. Ayachit, Chem. Phys. Lett. 164 (2–3) (1989) 253–260.
[15] N.H. Ayachit, Asian J. Phys. 9 (2000) 349.
[16] Y.F. Nadaf, D.K. Deshpande, A.M. Karaguppikar, S.R. Inamdar, J. Photosci. 9 (2002) 29.
[17] N.H. Ayachit, G. Neeraja Rani, Phys. Chem. Liq. 45 (1) (2007) 41–45.
[18] H. Trauble, H. Eibl, Proc. Natl. Acad. Sci. U. S. A. 71 (1974) 214.
[17] F. Bellemare, M. Fragata, J. Colloid Interface Sci. 77 (1980) 243.
[19] M. Fragata, F. Bellemare, J. Colloid Interface Sci. 107 (1985) 553.
[20] Y. Kimura, A. Ikegami, J. Membr. Biol. 85 (1985) 225.
[21] N.A. Nemkovich, A.N. Rubinov, M.G. Savvidi, Inst. Phys. Conf. Ser. 126 (1992) 639.
[22] N.A. Nemkovich, A.N. Rubinov, J. Fluoresc. 5 (1995) 285.
[23] N.A. Nemkovich, W. Baumann, J.V. Kruchenok, H. Reis, A.N. Rubinov, J. Fluoresc. 7 (1997) 363.
[24] N.R. Patil, R.M. Melavanki, S.B. Kapatkar, N.H. Ayachit, J. Saravanan, J. Fluoresc. 21 (3) (2011) 1213–1222.
[25] B.G. Evale, S.M. Hanagodimath, I.A. Khan, Spectrochim. Acta A 73 (2009) 694–700.
[26] S.P. Olivares, S. Risso, M.I. Gutierrez (Eds.),Spectrochim. Acta A 71 (2008) 336–339.
[27] J. Thipperudrappa, D.S. Biradar, S.R. Manohara, S.M. Hanagodimath, Spectrochim. Acta A 69 (3) (2008) 991–997.
[28] K. Chandrasekhar, L.R. Naik, H.M. Suresh Kumar, N.N. Math, Indian J. Pure Appl. Phys. 44 (2006) 292–299.
[29] K. Guzow, M. Milewska, W. Wiczk, Spectrochim. Acta A 61 (2005) 1133–1140.
[30] A. Kawski, J.F. Rabek (Eds.), Progress in Photochemistry and Photophysics, V, CRC Press, Boca Raton 1992, pp. 1–47.
[31] W. Liptay, E.C. Lim (Eds.), Excited States, vol. I, Academic Press, New York 1974, pp. 129–229.
[32] M.K. Saroj, N. Sharma, R.C. Rastogi, J. Mol. Struct. 1012 (2012) 73–86.
[33] R.M. Melavanki, N.R. Patil, S.B. Kapatkar, N.H. Ayachit, S. Umapathy, J. Thipperudrappa, A.R. Nataraju, J. Mol. Liq. 158 (2011) 105–110.
[34] M.S. Zakerhamidi, S.A. di-Kandjani, M. Moghadam, E. Ortyl, S. Kucharski, Spectrochim. Acta A Mol. Biomol. Spectrosc. 85 (2012) 105–110.
[35] Y.T. Varma, S. Joshi, D.D. Pant, J. Mol. Liq. 179 (2013) 7–11.
[36] J. Jayabharathi, V. Kalaiarasi, V. Thanikachalam, K. Jayamoorthy, J. Fluoresc. 24 (2014) 599–612.
[37] J.S. Kadadevarmath, G.H. Malimath, N.R. Patil, H.S. Geethanjali, R.M. Melavank, Can. J. Phys. 91 (2013) 1107–1113.
[38] S.D. Choudhury, S. Basu, Chem. Phys. Lett. 371 (2003) 136–140.
[39] A. Grofsik, M. Kubinyi, A. Ruzsinszky, T. Veszpremi, W.J. Jones, J. Mol. Struct. 555 (2000) 15–19.
[40] E. Lippert, Z. Naturforsch. 10 (1955) 541–545.
[41] N.G. Bakshiev, Opt. Spektrosk. 16 (1964) 821–832.
[42] A. Kawski, Z. Naturforsch. 57a (2002) 255–262.
[43] A. Chamma, P. Viallet, C. R. Acad. Sci. Paris Ser. C 270 (1970) 1901–1910.
[44] D.S. Chemla, J. Zyss, Non-linear Optical Properties of Organic Molecules and Crystals, Academic Press, New York, 1987.
[45] S. Joshi, D.D. Pant, J. Mol. Liq. 166 (2012) 49–52.
[46] S. Joshi, D.D. Pant, J. Mol. Liq. 172 (2012) 125–129.
[47] S. Joshi, R. Bhattacharjee, T. Varma, D.D. Pant, J. Mol. Liq. 179 (2013) 88–93.
[48] S. Joshi, S. Kumari, R. Bhattacharjee, R. Sakhuja, D.D. Pant, J. Mol. Liq. 200 (2014) 115–119.
[49] S. Joshi, S. Kumari, R. Bhattacharjee, R. Sakhuja, D.D. Pant, J. Mol. Liq. 209 (2015) 219–223.
[50] R. Sharma, S. Joshi, R. Bhattacharjee, D.D. Pant, J. Mol. Liq. 200 (2015) 159–164.
[51] H. Khanmohammadi, A. Abdollahi, Dyes Pigments 94 (2012) 163–168.
[52] R.M. El-Shishtawy, F. Borbone, Z.M. Al-amshany, A. Tuzi, A. Barsella, A.M. Asiri, A. Roviello, Dyes Pigments 96 (2013) 45–51.
[53] S. Salmani, M.H. Majles Ara, M.S. Zakerhamidi, E. Safari, Dyes Pigments 125 (2016) 132–135.
[54] M.S. Zakerhamidi, M. Keshavarz, H. Tajalli, A. Ghanadzadeh, S. Ahmadi, M. Moghadam, S.H. Hosseini, V. Hooshangi, J. Mol. Liq. 154 (2010) 94–101.
[55] N.G. Bakhshiev, Opt. Spektrosk. 16 (1964) 821–832.
[56] L. Bilot, A. Kawski, Z. Naturforsch. 17a (1962) 621–627.
[57] L. Bilot, A. Kawski, Z. Naturforsch. 18a (1963) 256–262.
[58] R. Yang, S. Peng, T.C. Hughes, Soft Matter 10 (2014) 2188–2196.
[59] P. Hohenberg, W. Kohn, Phys. Rev. B 136 (1964) 864–871.
[60] R.G. Parr, W. Yang, Density-Functional Theory of Atoms and Molecules, Oxford University Press, New York, 1989.
[61] M.J. Frisch, et al., Gaussian 09, Revision D.01, Gaussian, Inc., Wallingford, CT, 2009.
[62] (a) A.D. Becke, Phys. Rev. A 38 (1988) 3098–3100;
(b) C. Lee, W. Yang, R.G. Parr, Phys. Rev. B 37 (1988) 785–789.
[63] S. Miertuš, J. Tomasi, Chem. Phys. 65 (1982) 239–245.
[64] S. Miertuš, E. Scrocco, J. Tomasi, Chem. Phys. 55 (1981) 117–129.
[65] R. Dennington, T. Keith, J. Milam, GaussView, Version 5, Semichem Inc., Shawnee Mission KS, 2009.
[66] Y. Gülseven Sıdır, I_. Sıdır, E. Taßsal, E. Ermisß, Spectrochim. Acta A 78 (2011) 640–647.
[67] Y. Gülseven Sıdır, I_. Sıdır, H. Berber, E. Taßsal, J. Mol. Liq. 162 (2011) 148–154.
[68] I. Sıdır, Y. GülsevenSıdır, H. Berber, E. Taßsal, J. Mol. Liq. 178 (2013) 127–136.
[69] F.A.S. Chipem, A. Mishra, G. Krishnamoorthy, Phys. Chem. Chem. Phys. 14 (2012) 8775–8790.
[70] (a) T. Kupkaa, I.P. Gerothanassis, I.N. Demetropoulos, J. Mol. Struct. (THEOCHEM) 531 (2000) 143–157;
(b) M. Monajjemi, Z. Eslamifar, S.M. Shoaei, F. Mollaamin, Afr. J. Microbiol. Res. 6 (2012) 2338–2345.
[71] K.L. Bak, J. Gauss, T. Helgaker, P. Jørgensen, J. Olsen, Chem. Phys. Lett. 319 (2000) 563–568.